

## Lymph node mapping using quantum dot-labeled polymersomes

Rumiana Bakalova<sup>1,2</sup>, Zhiyko Zhelev<sup>1,3,4</sup>, Biliiana Nikolova<sup>3</sup>, Shuhei Murayama<sup>1</sup>, Desislava Lazarova<sup>2</sup>, Iana Tsoneva<sup>3</sup> and Ichio Aoki<sup>1</sup>

<sup>1</sup> *Molecular Imaging Center, National Institute of Radiological Sciences, 4-9-1 Anagawa, Inage-ku, Chiba 263-8555, Japan*

<sup>2</sup> *Medical Faculty, Sofia University, 1 Koziak Str., Sofia 1407, Bulgaria*

<sup>3</sup> *Institute of Biophysics and Biomedical Engineering, Bulgarian Academy of Sciences, Sofia 1113, Bulgaria*

<sup>4</sup> *Medical Faculty, Trakia University, 11 Armeiska Str., Stara Zagora 6000, Bulgaria*

**Abstract.** The present study was designed to investigate whether poly-ion complex hollow vesicles (polymersomes), based on chemically-modified chitosan, are appropriate for lymph node mapping in the context of their application in the development of theranostic nanosized drug delivery systems (nano-DDS). The experiments were performed on Balb/c nude mice (colon cancer-grafted). The mice were subjected to anesthesia and quantum dot (QD<sup>705</sup>)-labeled polymersomes (d~120 nm) were injected intravenously *via* the tail vein. The optical imaging was carried out on Maestro EX Imaging System (excitation filter: 435–480 nm; emission filter: 700 nm). A strong fluorescent signal, corresponding to QD<sup>705</sup> fluorescence, was detected in the lymph nodes, as well as in the tumor. A very weak fluorescent signal was found in the liver area. The half-life of QD<sup>705</sup>-labelled polymersomes was  $6 \pm 2$  hours in the bloodstream and  $11 \pm 3$  hours in the lymph nodes. The data suggest that polymersomes are very promising carriers for lymph node mapping using QD as a contrast agent. They are useful matrix for development of nano-formulations with theranostic capabilities.

**Key words:** Polymersomes — Quantum dot — Lymph nodes — Imaging

### Introduction

Lymph node targeting and mapping is a very important direction in the development of theranostic nanosized drug delivery systems (nano-DDS) due to the possibility to treat metastases and/or to visualize and remove the sentinel metastatic lymph nodes in surgery. The biopsy of the sentinel lymph nodes is very simple as a concept, but practically (technically) it is not so easy. In clinical practice, the most commonly used fluorophore for this purpose is isosulfan blue (Schaafsma et al. 2014). However, sometimes the sentinel lymph nodes could be located too deeply (to ~10 cm below the skin), which restricts their visualization and localization prior to surgery using conventional organic fluorophores. Therefore, each novelty in this methodology, that improves the technique, is accepted with a great enthusiasm by clinicians.

The fluorescent imaging using quantum dots (QDs) have a great potential for application in surgery – for a precise and fast localization of sentinel lymph nodes and small lesions (e.g., metastatic tumors), and facilitation of their removal. QDs allow visualization of the lymph nodes at a few centimeters below the skin surface, before proceeding to the resection. Thus, it is possible to reduce the size of the resection and to decrease the time of surgical intervention.

A lymph node mapping, using QDs, was first published in Nature Biotechnology (2004) by Bawendy and Frangioni's teams (Kim et al. 2004). Currently, there is no doubt about the clinical importance of this approach, especially in cancer therapy (Vahrmeijer et al. 2013). The near-infrared fluorescent nanoparticles have a real potential to replace the conventional organic fluorophores in the biopsy of the sentinel lymph nodes (Ashitate et al. 2014).

The selective disposition of nanocarriers into the target tissue is an essential issue in drug delivery and lymph node mapping. In the last several years, the critical size of nanocarriers (150 nm), discriminating the permeability into normal and tumor tissues, was determined by the use of size-tunable, polyion complex hollow vesicles (polymer-

Correspondence to: Rumiana Bakalova, Molecular Imaging Center, National Institute of Radiological Sciences (NIRS), 4-9-1 Anagawa, Inage-ku, Chiba 264-8555, Japan  
E-mail: bakalova@nirs.go.jp

somes) as a ruler (Meng et al. 2011; Bennett et al. 2014). Polymersomes are capable of encapsulating hydrophobic and hydrophilic drugs and they can be surface functionalized for target-selective drug delivery and delivery of imaging probes. Their polymeric membrane potentially offers a protective barrier to proteins, peptides, DNA and RNA fragments against deleterious factors that may be present in the biological environment (Bennett et al. 2014).

To evaluate the impact of polymersomes (made by different polymer matrices) as drug carriers, it is necessary to investigate their pharmacodynamics *in vivo* and especially the possibility to deliver them into the target tissues. One of the most preferred targets is cancer due to the efforts to develop highly specific therapeutic strategies with minimal side-effects. The polymersomes are usually labeled by different contrast agents and their pharmacodynamics in cancer and non-cancer tissues has investigated *in vivo* by optical imaging, magnetic resonance imaging, positron-emission tomography, multimodal imaging (Ghoroghchian et al. 2005; Duncan et al. 2008). Currently, a limited number of studies describe a localization of polymersomes (Tat-peptide or antigen-conjugated) in lymph nodes (Christian et al. 2009; Stano et al. 2013).

Semiconductor QDs are one of the most appropriate fluorescent markers for deep-tissue optical imaging of pharmacodynamics of polymersomes in living organisms (Kim et al. 2004; Bakalova et al. 2007). The unique optical properties of QDs can be used to optimize the signal-to-background ratio, to improve the sensitivity of fluorescence detection, and to increase the quality of fluorescent deep-tissue imaging *in vivo* (Kim et al. 2004; Bakalova et al. 2008). Moreover, single QDs can be observed and tracked for up to few hours by fluorescence confocal microscopy, total internal reflection microscopy, or basic wide-field epifluorescence microscopy,

and single-molecule microscopy, as well as up to few days by optical (fluorescent) imaging systems. QDs are also excellent probes for two/multi-photon confocal microscopy because they are characterized by a large absorption cross-section (Bakalova et al. 2011; Osakada and Cui 2011; Chang and Rosenthal 2013; Hafian et al. 2014).

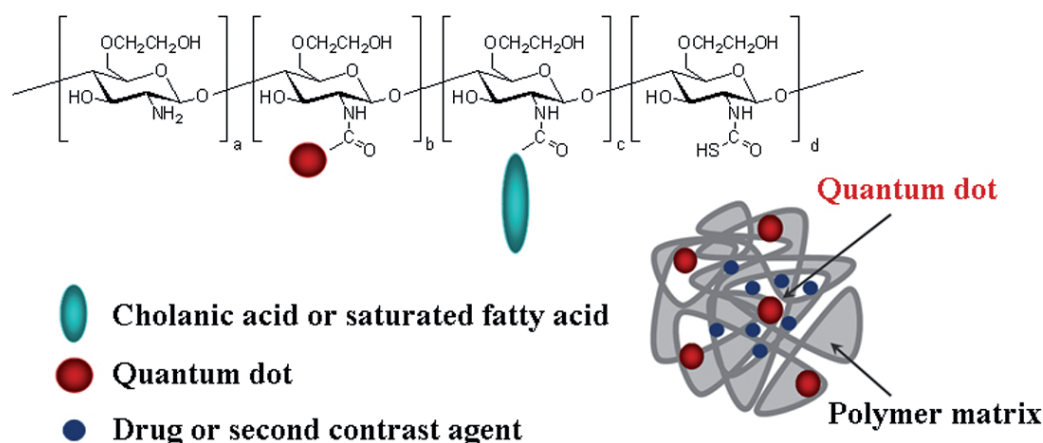
The present study was designed to investigate the possibility for lymph node mapping using QD-labeled size-controlled long-circulating polymersomes on experimental animals, visualized by fluorescent imaging *in vivo*, and to clarify their potential as a carrier of drugs and/or contrast agents in diagnostic and treatment of metastases.

## Materials and Methods

### Chemicals

Water-soluble polymersomes were prepared from cholanic acid-modified chitosan as it was described by Lee et al. (2012) – with slight modifications (QDs and saturated fatty acid were conjugated with chitosan, instead of siRNA). Labeling of polymersomes with QDs was carried out *via* carbodiimide chemistry, using N-(3-dimethylaminopropyl)-N'-ethylcarbodiimide hydrochloride (EDC) as a zero-length cross-linker (Hermanson 1996). The nanoparticles were characterized by transmission electron microscopy (TEM), dynamic light scattering (DLS) and fluorescent spectroscopy. The concentration of QDs in polymersomes was calculated by the method of Yu et al. (2003). The structure of the nanoparticles and their physicochemical characteristics are shown in Scheme 1.

QDot®705 ITK™ Carboxyl Quantum Dots were purchased from Invitrogen. Isoflurane was purchased from



**Scheme 1.** Scheme and physicochemical characteristics of QD-labeled polymersomes, based on chemically modified chitosan. Physicochemical characteristics of QD-labeled polymersomes: average size – 128 nm; size-distribution ~30%; excellent water-solubility; stability in high-salt physiological fluids (aggregation was not detected).

Abbott (Japan). All chemicals used in this study were of analytical or HPLC grade.

#### Experimental cancer model

Balb/c nude mice ( $21 \pm 2$  g) were used. Conol26 cells ( $1 \times 10^5$  in  $10 \mu\text{l}$  PBS, pH 7.4) were inoculated subdermally in the left/right hindpaw. All measurements were performed  $\sim 9$ – $10$  days after inoculation, when the tumour size was  $\sim 100 \text{ mm}^3$ .

All experiments were conducted in accordance with the guidelines of the Physiological Society of Japan and were approved by the Animal Care and Use Committee of the National Institute of Radiological Sciences, Chiba, Japan.

#### Optical imaging

All experiments *in vivo* were conducted under anaesthesia. Briefly, the mouse was anaesthetized with 1.5% isoflurane using mask. The tail vein was catheterized for administration of nanoparticles and the mouse was fixed in the camera of the Maestro EX Imaging System, connected to anaesthesia device. The body autofluorescence was registered at excitation filter 435–480 nm and emission filter 700 nm (longpass). Nanoparticles (QD<sup>705</sup> or QD<sup>705</sup>-labelled polymersomes) were injected intravenously (i.v.) *via* the tail vein (single dose – 80 nmol;  $100 \mu\text{l}$  volume) and the whole body fluorescence was registered on the back and stomach side at different

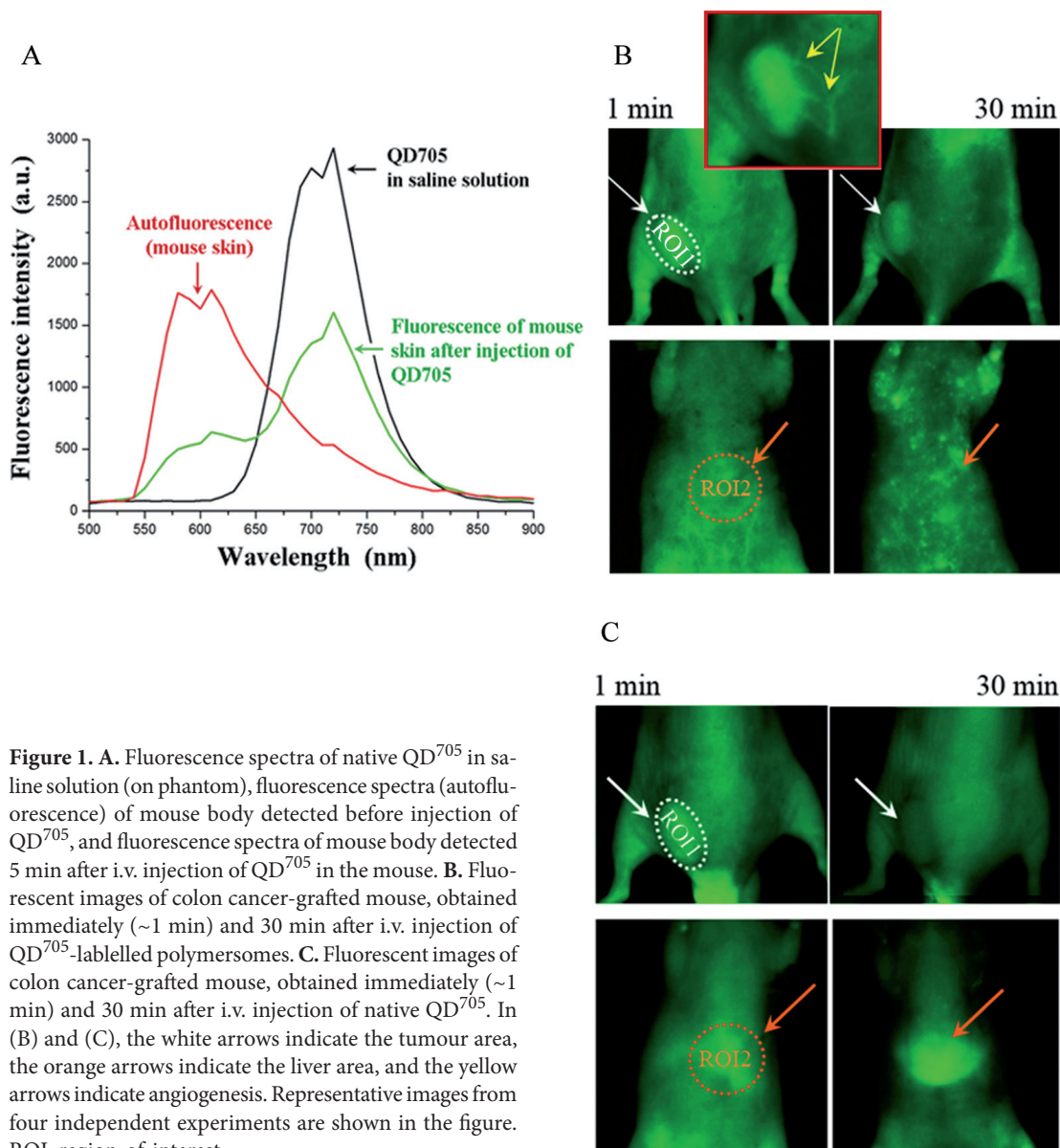


**Figure 1.** A. Fluorescence spectra of native QD<sup>705</sup> in saline solution (on phantom), fluorescence spectra (autofluorescence) of mouse body detected before injection of QD<sup>705</sup>, and fluorescence spectra of mouse body detected 5 min after i.v. injection of QD<sup>705</sup> in the mouse. B. Fluorescent images of colon cancer-grafted mouse, obtained immediately ( $\sim 1$  min) and 30 min after i.v. injection of QD<sup>705</sup>-labelled polymersomes. C. Fluorescent images of colon cancer-grafted mouse, obtained immediately ( $\sim 1$  min) and 30 min after i.v. injection of native QD<sup>705</sup>. In (B) and (C), the white arrows indicate the tumour area, the orange arrows indicate the liver area, and the yellow arrows indicate angiogenesis. Representative images from four independent experiments are shown in the figure. ROI, region-of-interest.

time-intervals. The data were analyzed by Living Image In Vivo Imaging software (Maestro version 2.10.0).

## Results and Discussion

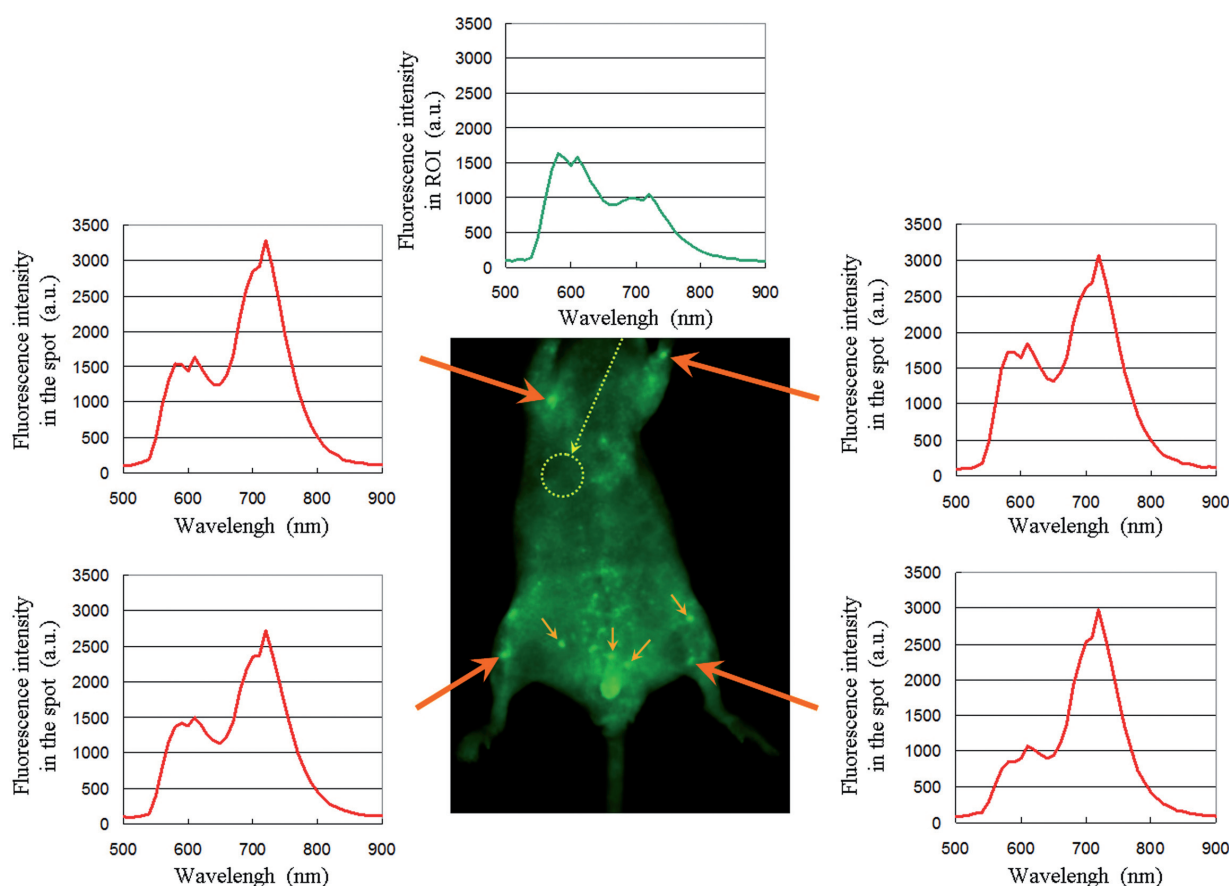
In preliminary experiment we selected the appropriate concentration of QD<sup>705</sup> for *in vivo* imaging, which gives a high signal-to-background ratio without saturation of the fluorescent signal and existence of artifacts. Thus, before fluorescent imaging on cancer-grafted mice, all imaging parameters were optimized using native QD<sup>705</sup> solutions in different concentrations, applied on phantoms and healthy mice (subcutaneous and intravenous injections in different volumes). The most optimal concentration of QD<sup>705</sup> for *in vivo* application was a single dose of ~80 nmol in 100  $\mu$ l volume.

Figure 1A shows the fluorescent spectra of native QD<sup>705</sup> in saline solution (black line), autofluorescence spectra of mouse body (red line) and their overlap after injection of native QD<sup>705</sup> in mouse *via* the tail vein (green line). The

data indicate that QD<sup>705</sup>, emitting in the near-infrared region of the spectrum (700–900 nm), allow to overcome the autofluorescence of mouse body and to obtain a strong fluorescent signal around 700–710 nm, which comes from the nanoparticles.

The images in Figure 1B,C were obtained on colon cancer-grafted mice, injected intravenously with QD<sup>705</sup>-labelled polymersomes or native QD<sup>705</sup> in a concentration, selected in preliminary experiments. The images were obtained immediately (~1 min) and 30 min after injection of the nanoparticles. In this short period after injection, the tumor was visualized on the basis of angiogenesis (yellow arrows) in both cases. The quantum yield of QD<sup>705</sup> was high enough to allow a deep-tissue imaging of blood vessels. The native QD<sup>705</sup> were rapidly accumulated into the liver, while QD<sup>705</sup>-labelled polymersomes practically were not detected in the liver area.

Bright fluorescent spots were visualized on the stomach side of the mice, injected with QD-labelled polymersomes (Figure 2). In all overlapped spectra detected in these spots, there was a very well-defined fluorescent maximum



**Figure 2.** Visualization of lymph nodes in colon cancer-bearing mouse after i.v. injection of QD<sup>705</sup>-labelled polymersomes. A representative image, obtained 30 min after injection is shown. The fluorescent spectra in red were obtained from each bright spot, indicated by orange arrows. The fluorescent spectrum in green was obtained from the region-of-interest (ROI), indicated by yellow dotted arrow.

at 705 nm, corresponding to the QD<sup>705</sup>. The background spectrum (green line) detected outside the spots was characterized by a high maximum at ~600 nm and a comparatively small maximum at 705 nm. In situ imaging showed that these were lymph nodes (data are not shown).

The half-life of fluorescence intensity of QD<sup>705</sup>-labelled polymersomes was  $6 \pm 2$  hours in the bloodstream and  $11 \pm 3$  hours in the lymph nodes. Maximum fluorescence intensity in the lymph nodes was detected on the 1<sup>st</sup> hours after injection, followed by a plateau within 3 hours and comparatively slow decrease within 3–24 hours (Figure 3). Weak fluorescent signal was detected in the liver area.

Recently, two teams only have reported a localization of size-controlled polymersomes (composed of different block copolymers) in lymph nodes. In 2009, Christian et al. have developed PZn<sub>3</sub>-labeled Tat-peptide conjugated NIR-emissive polymersomes composed of poly(ethylene oxide (1300)-*b*-butadiene(2500)) with 4-fluoro-3-nitrobenzoic acid (Christian et al. 2009). The polymersomes have been applied for *in vivo* dendritic cell tracking using fluorescence lifetime imaging. During the measurements the authors

have observed an accumulation of the fluorescent dye in the lymph nodes. In 2013, Stano et al. have described antigen-loaded polymersomes composed of poly(propylene sulfide) and poly(ethylene glycol) (Stano et al. 2013). The authors have observed that these nanoparticles induced enhanced frequencies of antigen-specific CD4<sup>+</sup> T cells in the spleen, lymph nodes and lungs. Our study is the first demonstrating a direct lymph node mapping using polymersomes conjugated with contrast agent (e.g., quantum dot).

The data suggest that size-controlled long-circulating polymersomes are very promising carriers for contrast substances in lymph node mapping and drug-carriers for treatment of metastases. They are useful matrix for development of nano-formulations with theranostic capabilities.

The growing number of studies on polymersomes shows that these nanoparticles are new and valuable tools for disease diagnosis and therapy. The enhanced stability and tunability of polymersomes will ultimately lead to the development of effective carriers for *in vivo* drug delivery, molecular imaging, and cellular mimicry. The potential to co-encapsulate two drug molecules in the same polymer-

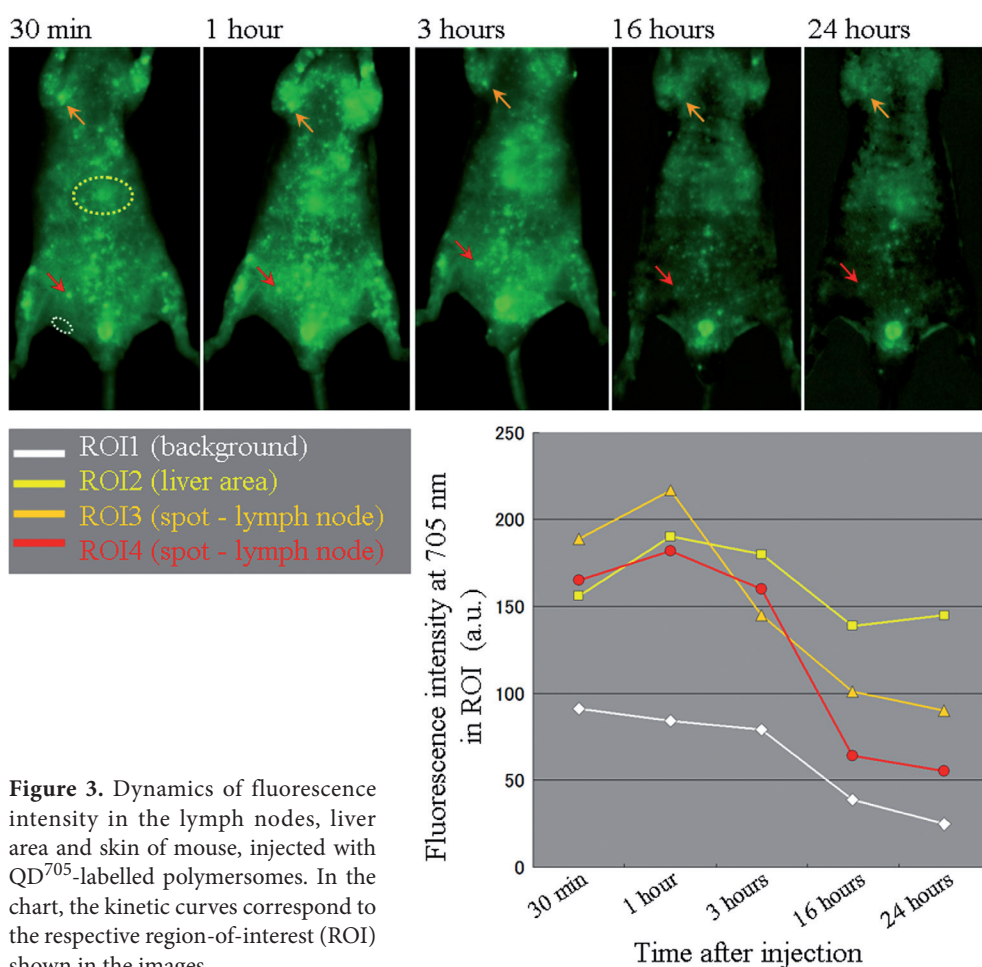


**Figure 3.** Dynamics of fluorescence intensity in the lymph nodes, liver area and skin of mouse, injected with QD<sup>705</sup>-labelled polymersomes. In the chart, the kinetic curves correspond to the respective region-of-interest (ROI) shown in the images.

some enables combination therapies and eliminates the need to individually administer two separate drug formulations (Levine et al. 2008; Chen et al. 2014).

**Acknowledgments.** The authors thank Ms. Sayaka Shibata (Molecular Imaging Center, National Institute of Radiological Sciences, Japan) for her assistance during the experiments *in vivo*. This study was partially supported by a grant-in-aid „Kakenhi” (No. 24510321) from the Ministry of Education, Science and Technology of Japan (granted to R. B.) and JSPS Fellowship (granted to B. N.).

**Conflict of interest.** The authors report no conflicts of interest in this work.

## References

- Ashitate Y., Hyun H., Kim S. H., Lee J. H., Henary M., Frangioni J. V., Choi H. S. (2014): Simultaneous mapping of pan and sentinel lymph nodes for real-time image-guided surgery. *Theranostics* **4**, 693–700  
<http://dx.doi.org/10.7150/thno.8721>
- Bakalova R., Zhelev Z., Aoki I., Kanno I. (2007): Designing quantum dot probes. *Nat. Photonics* **1**, 487–489  
<http://dx.doi.org/10.1038/nphoton.2007.150>
- Bakalova R., Zhelev Z., Gadjeva V. (2008): Quantum dots versus organic fluorophores in fluorescent deep-tissue imaging – merits and demerits. *Gen. Physiol. Biophys.* **27**, 231–242
- Bakalova R., Zhelev Z., Kokuryo D., Spasov L., Aoki I., Saga T. (2011): Chemical nature and structure of organic coating of quantum dots is crucial for their application in imaging diagnostics. *Int. J. Nanomedicine* **6**, 1719–1732  
<http://dx.doi.org/10.2147/IJN.S17995>
- Bennett K. M., Jo J., Cabral H., Bakalova R., Aoki I. (2014): MR imaging techniques for nano-pathophysiology and theranostics. *Adv. Drug Deliv. Rev.* **74**, 75–94  
<http://dx.doi.org/10.1016/j.addr.2014.04.007>
- Chang J. C., Rosenthal S. J. (2013): Quantum dot-based single-molecule microscopy for the study of protein dynamics. *Methods Mol. Biol.* **1026**, 71–84  
[http://dx.doi.org/10.1007/978-1-62703-468-5\\_6](http://dx.doi.org/10.1007/978-1-62703-468-5_6)
- Chen W., Meng F., Cheng R., Deng C., Feijen J., Zhong Z. (2014): Advanced drug and gene delivery systems based on functional biodegradable polycarbonates and copolymers. *J. Control. Release* **190**, 398–414  
<http://dx.doi.org/10.1016/j.jconrel.2014.05.023>
- Christian N. A., Benencia F., Milone M. C., Li G., Frail P. R., Therien M. J., Coukos G., Hammer D. A. (2009): In vivo dendritic cell tracking using fluorescence lifetime imaging and near-infrared-emissive polymersomes. *Mol. Imaging Biol.* **11**, 167–177  
<http://dx.doi.org/10.1007/s11307-008-0184-x>
- Duncan T. V., Ghoroghchian P. P., Rubstov I. V., Hammer D. A., Therien M. J. (2008): Ultrafast excited-state dynamics of nanoscale near-infrared emissive polymersomes. *J. Am. Chem. Soc.* **130**, 9773–9784  
<http://dx.doi.org/10.1021/ja711497w>
- Ghoroghchian P. P., Frail P. R., Susumi K., Blessington D., Branman A. K., Bates F. S., Chance B., Hammer D. A., Therien M. J. (2005): Near-infrared-emissive polymersomes: self-assembled soft matter for in vivo optical imaging. *Proc. Natl. Acad. Sci. USA* **102**, 2922–2977  
<http://dx.doi.org/10.1073/pnas.0409394102>
- Hafian H., Sukhanova A., Turini M., Chames P., Baty D., Pluot M., Cohen J. H., Nabiev I., Millot J. M. (2014): Multiphoton imaging of tumour biomarkers with conjugates of single-domain antibodies and quantum dots. *Nanomedicine* **10**, 1701–1709  
<http://dx.doi.org/10.1016/j.nano.2014.05.014>
- Hermanson G. T. (1996): *Bioconjugate Techniques*. Academic Press, New York
- Kim S., Lim Y. T., Soltesz E. G., De Grand A. M., Lee J., Nakayama A., Parker J. A., Mihaljevic T., Laurence R. G., Dor D. M., et al. (2004): Near-infrared fluorescent type II quantum dots for sentinel lymph node mapping. *Nat. Biotechnol.* **22**, 93–97  
<http://dx.doi.org/10.1038/nbt920>
- Lee S. J., Huh M. S., Lee S. Y., Min S., Lee S., Koo H., Chu J.-U., Lee K. E., Jeon H., Choi Y., et al. (2012): Tumor-homing poly-siRNA/glycol chitosan self-cross-linked nanoparticles for systemic siRNA delivery in cancer treatment. *Angew. Chem. Int. Ed. Engl.* **51**, 7203–7207  
<http://dx.doi.org/10.1002/anie.201201390>
- Levine D. H., Ghoroghchian P. P., Freudenberg J., Zhang G., Therien M. J., Greene M. I., Hammer D. A., Murali R. (2008): Polymersomes: A new multi-functional tool for cancer diagnosis and therapy. *Methods* **46**, 25–32  
<http://dx.doi.org/10.1016/j.ymeth.2008.05.006>
- Meng H., Xue M., Xia T., Ji Z., Tarn D. Y., Zink J. I., Nel A. E. (2011): Use of size and a copolymer design feature to improve the biodistribution and the enhanced permeability and retention effect of doxorubicin-loaded mesoporous silica nanoparticles in a murine xenograft tumor model. *ACS Nano* **5**, 4131–4144  
<http://dx.doi.org/10.1021/nn200809t>
- Osakada Y., Cui B. (2011): Real-time visualization of axonal transport in neurons. *Methods Mol. Biol.* **670**, 231–243  
[http://dx.doi.org/10.1007/978-1-60761-744-0\\_16](http://dx.doi.org/10.1007/978-1-60761-744-0_16)
- Schaafsma B. E., Verbeek F. P., Elzevier H. W., Tummers Q. R., van der Vorst J. R., Frangioni J. V., van de Velde C. J., Pelger R. C., Vahrmeijer A. L. (2014): Optimization of sentinel lymph node mapping in bladder cancer using near-infrared fluorescence imaging. *J. Surg. Oncol.* **110**, 845–850  
<http://dx.doi.org/10.1002/jso.23740>
- Stano A., Scott E. A., Dane K. Y., Swartz M. A., Hubell J. A. (2013): Tunable T cell immunity towards a protein antigen using polymersomes vs. solid-core nanoparticles. *Biomaterials* **34**, 4339–4346  
<http://dx.doi.org/10.1016/j.biomaterials.2013.02.024>
- Yu W. W., Qu L., Guo W., Peng X. (2003): Experimental determination of the extinction coefficient of CdTe, CdSe, and CdS nanocrystals. *Chem. Mater.* **15**, 2854–2860  
<http://dx.doi.org/10.1021/cm034081k>
- Vahrmeijer A. L., Hutteman M., van der Vorst J. R., van de Velde C. J., Frangioni J. V. (2013): Image-guided cancer surgery using near-infrared fluorescence. *Nat. Rev. Clin. Oncol.* **10**, 507–518  
<http://dx.doi.org/10.1038/nrclinonc.2013.123>

Received: December 2, 2014

Final version accepted: February 20, 2015

First published online: July 29, 2015